Embedding formulae for wave diffraction by a circular arc

Article

Accepted Version

It is advisable to refer to the publisher's version if you intend to cite from the work. See Guidance on citing.

www.reading.ac.uk/centaur

CentAUR

Embedding formulae for wave diffraction by a circular arc

C.A.J. Moran[a], N.R.T. Biggs[a,*], P.G. Chamberlain[a]

[a]*Department of Mathematics and Statistics, School of Mathematical and Physical Sciences, University of Reading, P.O. Box 220, Whiteknights, Reading RG6 6AX, United Kingdom*

Abstract

For certain wave diffraction problems, embedding formulae can be derived, which represent the solution (or far-field behaviour of the solution) for all plane wave incident angles in terms of solutions of a (typically small) set of other auxiliary problems. Thus a complete characterisation of the scattering properties of an obstacle can be determined by only determining the solutions of the auxiliary problems, and then implementing the embedding formula. The class of scatterers for which embedding formulae can be derived has previously been limited to obstacles with piecewise linear boundaries; here this class is extended to include a simple curved obstacle, consisting of a thin circular arc. Approximate numerical calculations demonstrate the accuracy of the new embedding formulae.

Keywords: waves, diffraction, embedding, circular arc

1. Introduction

To fully characterise the wave scattering properties of an obstacle, solutions may be required for a range of plane wave incident angles. Embedding formulae are a means of reducing the effort required to achieve this full characterisation. These formulae express the solution or the far-field behaviour of the solution for an arbitrary incident wave angle in terms of analogous properties of a typically

---

*Corresponding author. *Email address:* n.r.t.biggs@reading.ac.uk

small set of other solutions. Thus once the problem is solved for this set of solutions the full characterisation follows immediately from the embedding formula without need to solve any further problems.

Embedding formulae were first derived in [1] and [2]. These papers showed that the solution for a plane wave incident at any angle upon a two-dimensional, thin, straight barrier containing a single gap, can be fully determined from the single solution corresponding to grazing plane wave incidence. Following [2], subsequent extensions [3-6] required the boundary-value problem to be formulated as an integral equation; the derivation of the embedding formulae then exploited the structure of the integral equation, and expressed the solution for arbitrary plane wave incident angle in terms of solutions corresponding to other plane wave incident angles. This approach was generalised in [7] in which a generalised integral equation problem, divorced from a particular wave diffraction interpretation, was addressed.

The papers [8,9] instead derived embedding formulae directly from the boundary-value problem, without recourse to an integral equation formulation, and expressed the far-field of the solution for arbitrary plane wave incident angle in terms of the far-field of solutions corresponding to particular multipole forcing at the corners of the scatterers. The method was generalised to certain three-dimensional scattering problems in [10]. In many ways this approach is more versatile as the problem does not need to first be formulated as an integral equation, but the calculation of the particular solutions required for the embedding formula which are forced by source terms at the scatterer corners may not be straightforward. To address this, [11-12] modified the boundary-value problem approach to allow the far-field of the solution for arbitrary plane wave incident angle to be expressed in terms of the far-field of solutions corresponding to other plane wave incident angles.

The class of scatterers for which embedding formulae have been derived thus far is rather limited: the scatterer boundaries must be piecewise linear, with each linear portion of the boundary oriented at a rational angle (i.e. $m\pi/n$, for integers m, n) to the x-axis (say). In the current paper we extend this class of

scatterers to a canonical scatterer in polar coordinates consisting of a circular arc.

Similar diffraction problems have been considered previously, though not within the context of embedding formulae. In [13] a model of a coastal harbour as a circular basin semi-embedded in an infinite coastline was developed, formulating the problem as an integral equation posed on the harbour opening and using a variational principle to provide an approximate solution. The case of porous harbour walls was considered in [14]. The problem of an electromagnetic plane wave incident upon an infinitely long, conducting, slotted cylinder is mathematically similar, and was solved numerically in [15]. In [16], the diffraction of a plane wave by precisely the scatterer geometry of the present paper was considered, though the investigation was limited to cases for which the entrance to the inner circular region was narrow, and focused on resonance excitation. More recently, [17] considered the scattering of a plane wave by a semi-circular inclusion in an otherwise infinite straight barrier.

The paper proceeds as follows. In section 2 the boundary-value problem is introduced. In section 3 a selection of embedding formulae are derived, firstly by adapting the approach of [11] to address the boundary-value problem directly, and then by reformulating the boundary-value problem as an integral equation, and using the results of [7] to exploit its structure. In each case the initial step is to decompose the incident plane wave $\phi_i^\alpha(r, \theta) = e^{ikr\cos(\theta-\alpha)}$ into an infinite sum and then consider the problem forced by an arbitrary term in this sum (referred to below as the 'modal problem'). Approximate numerical calculations are carried out in section 4, and a comparison is made between results determined from a direct approximation and via the embedding formulae. Finally, some conclusions and possible extensions are offered in section 5.

2. The boundary-value problem

The scatterer takes the shape of a portion of a circular arc (see fig. 1). Thus, in terms of standard polar coordinates (r, θ), the scatterer occupies the region

$$B = \{(r, \theta) : r = a, \ \theta \in [-\pi, \pi) \backslash (-\theta_1, \theta_1)\}, \tag{2.1}$$

in which $a > 0$ and $\theta_1 \in (0, \pi)$ are specified constants. The gap in the barrier is without loss of generality symmetrically oriented about the line $\theta = 0$. Throughout this paper we will refer to the domain for which $r < a$ as being 'within the arc', and $r > a$ as 'outside the arc'.

We suppose that there is a potential $\phi^\alpha(r, \theta)$ satisfying the Helmholtz equation

$$\frac{\partial^2 \phi^\alpha}{\partial r^2} + r^{-1} \frac{\partial \phi^\alpha}{\partial r} + r^{-2} \frac{\partial^2 \phi^\alpha}{\partial \theta^2} + k^2 \phi^\alpha = 0 \quad \text{in } \mathbb{R}^2 \backslash B. \tag{2.2}$$

Here k is the (specified) wavenumber, and the superscript α refers to the fact that ϕ^α includes a plane wave

$$\phi_{\mathrm{i}}^\alpha = e^{ikr \cos(\theta - \alpha)} \tag{2.3}$$

of unit amplitude and whose propagation direction makes an angle $\alpha \in [-\pi, \pi)$ with the positive x-axis, which is incident upon B. The incident plane wave has the expansion

$$\phi_{\mathrm{i}}^\alpha(r, \theta) = \sum_{n=-\infty}^{\infty} i^n J_n(kr) e^{in(\theta - \alpha)} \tag{2.4}$$

(see equation (2.77) in [18]), where J_n denotes the Bessel function of the first kind and order n.

The barrier B is 'hard', in the sense that the potential ϕ^α satisfies a homogeneous Neumann condition on the scatterer:

$$\frac{\partial \phi^\alpha}{\partial r} = 0 \quad \text{on } B. \tag{2.5}$$

For convenience, we decompose the potential ϕ^α outside the arc into the sum of the incident wave ϕ_{i}^α and a diffracted component ϕ_{d}^α:

$$\phi^\alpha(r, \theta) = \phi_{\mathrm{i}}^\alpha(r, \theta) + \phi_{\mathrm{d}}^\alpha(r, \theta) \quad \text{in } r > a. \tag{2.6}$$

4

The diffracted potential ϕ_d^α satisfies the Sommerfeld radiation condition

$$\lim_{r\to\infty} r^{1/2}\left(\frac{\partial \phi_d^\alpha}{\partial r} - ik\phi_d^\alpha\right) = 0, \tag{2.7}$$

uniformly in θ. Lastly, we require that the so-called Meixner or edge condition (e.g. [19]) holds, that is, if ρ measures distance from either corner of B, i.e. (a, θ_1) or $(a, -\theta_1)$, then here

$$\frac{\partial \phi^\alpha}{\partial \rho} = O(\rho^{-1/2}). \tag{2.8}$$

This condition ensures that energy is not added to the system at these points.

The boundary-value problem described above models, for example, surface gravity waves on fluid of uniform depth containing a surface-piercing structure of cross-section B, or three-dimensional acoustic waves in a medium containing an infinitely long structure of cross-section B.

The far-field behaviour of the solution as $kr \to \infty$ is of particular interest. We write

$$\phi_d^\alpha(r,\theta) = \sqrt{\frac{2}{\pi kr}} e^{i(kr-\pi/4)} F(\theta,\alpha) + O((kr)^{-3/2}), \tag{2.9}$$

where $F(\theta, \alpha)$ is referred to as the far-field diffraction coefficient, and θ as the observation angle. The far-field diffraction coefficient satisfies the well-known reciprocity principle (see e.g. [18])

$$F(\theta + \pi, \alpha) = F(\alpha + \pi, \theta), \tag{2.10}$$

and because of the symmetry of the scatterer B about the line $\theta = 0$ it is also clear that $\phi_d^\alpha(r,\theta) = \phi_d^{-\alpha}(r,-\theta)$ and so

$$F(\theta, \alpha) = F(-\theta, -\alpha). \tag{2.11}$$

3. Embedding formulae

Typically derivation of embedding formulae initially follows one of two distinct but related routes: either a particular differential operator is used, which commutes with the Helmholtz operator, boundary conditions, and radiation

condition, and annihilates the incident wave; or else the boundary-value problem is reformulated as an integral equation, and its structure is exploited. In section 3.1 we first use the differential operator approach, and then in section 3.2 derive an equivalent integral equation formulation and make use of its structure to derive complementary results.

3.1. From the boundary-value problem

For the scattering geometry B the simple operator

$$D = \frac{\partial}{\partial \theta} + \text{const.} \times I$$

certainly commutes with the Helmholtz operator $\partial^2/\partial r^2 + r^{-1}\partial/\partial r + r^{-2}\partial^2/\partial \theta^2 + k^2 I$, the boundary conditions (since the differentiation in D is in a direction parallel to the scatterer B), and also the radiation condition, but $D\phi_i^\alpha \neq 0$. However, the incident plane wave ϕ_i^α has the expansion (2.4), which can be written as

$$\phi_i^\alpha(r,\theta) = \sum_{n=-\infty}^{\infty} i^n e^{-in\alpha} \phi_i^n(r,\theta), \tag{3.1}$$

where

$$\phi_i^n(r,\theta) = J_n(kr)e^{in\theta} \qquad (n \in \mathbb{Z}), \tag{3.2}$$

and now the operator

$$D_n = \frac{\partial}{\partial \theta} - inI, \quad (n \in \mathbb{Z}) \tag{3.3}$$

is such that $D_n\phi_i^n = 0$ for all $n \in \mathbb{Z}$. This property suggests we decompose the solution ϕ^α as

$$\phi^\alpha(r,\theta) = \sum_{n=-\infty}^{\infty} i^n e^{-in\alpha} \phi^n(r,\theta) \tag{3.4}$$

where the solution corresponding to the forcing ϕ_i^n is denoted by ϕ^n, and then seek embedding formulae for solutions of this 'modal problem'. Once such formulae are derived, quantities related to the full solution ϕ^α can be reconstructed via (3.4).

Note that the operator D_n in (3.3) is very similar in form to the basic operator H used in [8], the only substantial difference being that there $\partial/\partial\theta$

is replaced by $\partial/\partial x$ and/or $\partial/\partial y$, because that work involved scatterers with straight edges.

We isolate the forcing ϕ_i^n from ϕ^n via the decomposition

$$\phi^n(r,\theta) = \phi_i^n(r,\theta) + \phi_d^n(r,\theta) \quad \text{in } \mathbb{R}^2 \backslash B; \tag{3.5}$$

comparison of (2.6) and (3.5), and use of (3.1) and (3.4), then shows that

$$\phi_d^\alpha(r,\theta) = \sum_{n=-\infty}^{\infty} i^n e^{-in\alpha} \phi_d^n(r,\theta) \quad \text{for } r > a. \tag{3.6}$$

We write

$$\phi_d^n(r,\theta) = \sqrt{\frac{2}{\pi kr}} e^{i(kr-\pi/4)} F_n(\theta) + O((kr)^{-3/2}) \tag{3.7}$$

as $kr \to \infty$, with

$$F_n(\theta) = \sum_{m=-\infty}^{\infty} f_{n,m} e^{im\theta}, \quad f_{n,m} = \frac{1}{2\pi} \int_{-\pi}^{\pi} F_n(\theta) e^{-im\theta} \, d\theta \qquad (n, m \in \mathbb{Z}). \tag{3.8}$$

Note that a consequence of (2.9) and (3.6)-(3.8) is that

$$F(\theta,\alpha) = \sum_{n=-\infty}^{\infty} i^n e^{-in\alpha} F_n(\theta) = \sum_{n=-\infty}^{\infty} i^n e^{-in\alpha} \sum_{m=-\infty}^{\infty} f_{n,m} e^{im\theta}. \tag{3.9}$$

3.1.1. Embedding formulae for the modal problem

The operator D_n in (3.3) commutes with the Helmholtz operator, the boundary conditions, and the radiation condition, and $D_n\phi_i^n = 0$ for $n \in \mathbb{Z}$. It also introduces so-called 'overly-singular' behaviour at the arc corners $(a, \pm\theta_1)$. To see this, first note that separation of variables applied local to a corner shows that a solution consistent with the Meixner condition (2.8) has the behaviour

$$\phi^n = A_0^n + A_1^n \rho^{1/2} \cos[(\sigma - \pi)/2] + O(\rho^{3/2}),$$

where ρ is the distance from the corner, and σ is the local azimuthal coordinate aligned so that $\sigma = 0$ points parallel to and away from the barrier (so $\sigma = \pm\pi$ locally coincides with the barrier). Here A_0^n and A_1^n are constants which depend on n.

Written in terms of the coordinates local to the corner at (a, θ_1), the differential operator D_n is

$$D_n = -a\cos\sigma \, \frac{\partial}{\partial\rho} + (1 + a\rho^{-1}\sin\sigma)\frac{\partial}{\partial\sigma} - inI,$$

so

$$D_n\phi^n = -\frac{1}{2}aA_1^n\rho^{-1/2}\cos[(\sigma+\pi)/2] + O(1)$$

as $k\rho \to 0$, and thus there is one overly singular term at this corner produced by the action of D_n. Application of D_n to the solution local to the corner at $(a, -\theta_1)$ yields a further overly-singular term. Thus we introduce the combination

$$\Phi = D_n\phi^n - (B_1 D_p\phi^p + B_2 D_q\phi^q),$$

where $n, p, q \in \mathbb{Z}$ are distinct, and the constants B_1 and B_2 are chosen so that the combination Φ is $O(1)$ at each corner. Then Φ satisfies the Helmholtz equation, a homogeneous boundary condition on B, the radiation condition, contains no forcing term, and is $O(1)$ at the arc corners, i.e. Φ satisfies a fully homogeneous boundary-value problem. The uniqueness of the scattering problem then implies that $\Phi \equiv 0$, so that

$$D_n\phi^n = B_1 D_p\phi^p + B_2 D_q\phi^q. \tag{3.10}$$

Solving (3.10) would provide an expression for ϕ^n in terms of ϕ^p and ϕ^q, but establishing the values of the 'constants' of integration is not straightforward, so we defer the derivation of this sort of embedding formula until section 3.2, calculated via the integral equation formulation.

Instead, we focus on deriving an embedding formula for the far-field coefficients. Let $kr \to \infty$ in (3.10). Using the notation of (3.7), the balance between leading order terms is

$$F_n' - inF_n = B_1(F_p' - ipF_p) + B_2(F_q' - iqF_q),$$

where F_n' denotes the θ-derivative of $F_n(\theta)$ and so on. Using the notation of (3.8), this becomes

$$\sum_{m=-\infty}^{\infty} (m-n)f_{n,m}e^{im\theta} = B_1 \sum_{m=-\infty}^{\infty} (m-p)f_{p,m}e^{im\theta} + B_2 \sum_{m=-\infty}^{\infty} (m-q)f_{q,m}e^{im\theta},$$

8

and so

$$(m-n)f_{n,m} = B_1(m-p)f_{p,m} + B_2(m-q)f_{q,m} \qquad (m \in \mathbb{Z}). \qquad (3.11)$$

This equality holds irrespective of the choice of m, so in particular setting $m = -p$ and $m = -q$ in turn shows that

$$(p+n)f_{n,-p} = 2pB_1 f_{p,-p} + B_2(p+q)f_{q,-p}, \ (q+n)f_{n,-q} = B_1(p+q)f_{p,-q} + 2qB_2 f_{q,-q},$$

from which

$$B_1 = \frac{\hat{f}_{q,-q}\hat{f}_{n,-p} - \hat{f}_{q,-p}\hat{f}_{n,-q}}{\hat{f}_{p,-p}\hat{f}_{q,-q} - \hat{f}_{p,-q}\hat{f}_{q,-p}}, \ \ B_2 = \frac{\hat{f}_{p,-p}\hat{f}_{n,-q} - \hat{f}_{p,-q}\hat{f}_{n,-p}}{\hat{f}_{p,-p}\hat{f}_{q,-q} - \hat{f}_{p,-q}\hat{f}_{q,-p}},$$

where for convenience we have written

$$\hat{f}_{p,q} = (p-q)f_{p,q} \qquad (p,q \in \mathbb{Z}). \qquad (3.12)$$

These representations for B_1, B_2 then allow (3.11) to be rewritten as

$$\hat{f}_{n,m} = \frac{(\hat{f}_{q,-q}\hat{f}_{n,-p} - \hat{f}_{q,-p}\hat{f}_{n,-q})\hat{f}_{p,m} + (\hat{f}_{p,-p}\hat{f}_{n,-q} - \hat{f}_{p,-q}\hat{f}_{n,-p})\hat{f}_{q,m}}{\hat{f}_{p,-p}\hat{f}_{q,-q} - \hat{f}_{p,-q}\hat{f}_{q,-p}} \qquad (3.13)$$

for $m \in \mathbb{Z}$.

Equation (3.13) is an expression for the modal far-field coefficient $(n - m)f_{n,m}$, but to serve as an embedding formula the right-hand side should depend only on quantities involving ϕ^p and ϕ^q. Reference to (3.8) and (3.9) shows that coefficients in (3.13) with first subscript p or q are acceptable in this sense, but coefficients with first subscript n are not. However, a form of reciprocity principle can be used to replace such terms by quantities which depend only on ϕ^p and ϕ^q. The full reciprocity principle is given in (2.10), which, given (3.8) and (3.9), can be expressed as

$$\sum_{n=-\infty}^{\infty} i^n e^{-in\alpha} \sum_{m=-\infty}^{\infty} f_{n,m} e^{im(\theta+\pi)} = \sum_{p=-\infty}^{\infty} i^p e^{-ip\theta} \sum_{q=-\infty}^{\infty} f_{p,q} e^{iq(\alpha+\pi)}.$$

Multiply this equation by $e^{i(j\theta-l\alpha)}$, for integers j, l, and integrate over $\alpha, \theta \in [-\pi, \pi]$: the orthogonality of the exponential functions on this interval shows that

$$f_{j,l} = i^{j+l} f_{-l,-j} \qquad (j,l \in \mathbb{Z}), \qquad (3.14)$$

9

in terms of which $\hat{f}_{j,l} = i^{j+l}\hat{f}_{-l,-j}$.

Using (3.14), equation (3.13) can then be written as

$$i^{-n}\hat{f}_{n,m} = \frac{(i^{-p}\hat{f}_{q,-q}\hat{f}_{p,-n} - i^{-q}\hat{f}_{q,-p}\hat{f}_{q,-n})\hat{f}_{p,m} + (i^{-q}\hat{f}_{p,-p}\hat{f}_{q,-n} - i^{-p}\hat{f}_{p,-q}\hat{f}_{p,-n})\hat{f}_{q,m}}{\hat{f}_{p,-p}\hat{f}_{q,-q} - \hat{f}_{p,-q}\hat{f}_{q,-p}}$$

(3.15)

the right-hand side of which now only requires knowledge of the far-field be-haviour of the two solutions ϕ^p, ϕ^q for its calculation. Here p, q are arbi-trary distinct but non-zero integers. An obvious choice is $q = -p$, for then $\hat{f}_{q,-p} = \hat{f}_{p,-q} = 0$, from (3.12), and (3.15) reduces to

$$i^{-n}\hat{f}_{n,m} = \frac{i^{-p}\hat{f}_{-p,p}\hat{f}_{p,-n}\hat{f}_{p,m} + i^{p}\hat{f}_{p,-p}\hat{f}_{-p,-n}\hat{f}_{-p,m}}{\hat{f}_{p,-p}\hat{f}_{-p,p}}.$$

(3.16)

One further simplification is possible due to the symmetry of B around $\theta = 0$, and the resulting modal symmetry property

$$f_{j,l} = (-1)^j f_{-j,-l} \qquad (j, l \in \mathbb{Z}),$$

(3.17)

which follows from the full symmetry property (2.11) in a similar fashion to how (3.14) stems from (2.10). Then $\hat{f}_{j,l} = (-1)^{j+1}\hat{f}_{-j,-l}$, and use of this reduces (3.16) to

$$\hat{f}_{p,-p}\hat{f}_{n,m} = i^{n-p}(\hat{f}_{p,-n}\hat{f}_{p,m} - \hat{f}_{p,n}\hat{f}_{p,-m}).$$

(3.18)

Here the coefficient $f_{n,m}$ (for $n \neq m$) associated with the solution ϕ^n is now expressed solely in terms of coefficients which depend only on the single solution ϕ^p, for $p \neq 0$. Both sides of (3.18) are zero if $m = n$, and in this case we can use L'Hôpital's rule to define

$$f_{n,n} = \lim_{m \to n} \frac{\partial}{\partial m}\left(\frac{-i^{n-p}(\hat{f}_{p,-n}\hat{f}_{p,m} - \hat{f}_{p,n}\hat{f}_{p,-m})}{\hat{f}_{p,-p}}\right).$$

(3.19)

Here derivatives with respect to m can be evaluated via (3.8); evaluation of the right-hand side of (3.19) still only requires knowledge of the single solution ϕ^p.

Equation (3.18) is thus an embedding formula, in that it expresses the modal far-field coefficient $f_{n,m}$ for all $n, m \in \mathbb{Z}$ in terms of coefficients which require knowledge of just ϕ^p for their calculation, for one value of $p \in \mathbb{Z}$. Furthermore,

10

using equation (3.9), which expresses the far-field diffraction coefficient $F(\theta, \alpha)$ for the full problem in terms of the modal far-field coefficient $f_{n,m}$, this means that $F(\theta, \alpha)$ can be calculated for *all* $\theta, \alpha \in [-\pi, \pi)$ once the single solution ϕ^p is determined, for any non-zero $p \in \mathbb{Z}$, and its far-field behaviour calculated.

3.2. From an integral equation formulation

In this section we formulate the boundary-value problem as an integral equation, and use the structure of this equation to re-derive and extend the embedding formulae determined in section 3.1.

An appropriate expression for the potential inside the arc is given by

$$\phi^\alpha(r, \theta) = \sum_{n=-\infty}^{\infty} a_n J_n(kr) e^{in\theta} \qquad (r < a, -\pi \le \theta < \pi), \qquad (3.20)$$

where J_n denotes the Bessel function of the first kind of order n, and the a_n are coefficients to be determined. These coefficients depend on α but in the interests of notational clarity this dependence is not made explicit.

The radial derivative of this expression, evaluated on B_0, is

$$\frac{\partial \phi^\alpha}{\partial r}(a^-, \theta) = \sum_{n=-\infty}^{\infty} k a_n J_n' e^{in\theta} \qquad (-\pi \le \theta < \pi),$$

where we adopt the convention that if the argument of a Bessel (or later Hankel) function is omitted then it is to be evaluated at ka, so $J_n' = J_n'(ka)$ etc. The orthogonality of the complex exponentials shows that

$$a_n = \frac{1}{2\pi k J_n'} \int_{-\theta_1}^{\theta_1} \frac{\partial \phi^\alpha}{\partial r}(a^-, \theta_0) e^{-in\theta_0} \, \mathrm{d}\theta_0 \qquad (n \in \mathbb{Z}) \qquad (3.21)$$

where the boundary condition (2.5) has been used to reduce the range of integration in (3.21) to the gap $(-\theta_1, \theta_1)$. For convenience, we introduce the notation

$$v^\alpha(\theta) = \frac{\partial \phi^\alpha}{\partial r}(a^\pm, \theta) \qquad (-\theta_1 < \theta < \theta_1), \qquad (3.22)$$

where it is implicit in this definition that $\partial \phi^\alpha / \partial r$ is continuous across the gap. Then inserting (3.21) into (3.20) shows that the potential within the arc can be

expressed as

$$\phi^\alpha(r,\theta) = \sum_{n=-\infty}^{\infty} \frac{J_n(kr)}{2\pi k J_n'} \int_{-\theta_1}^{\theta_1} v^\alpha(\theta_0) e^{in(\theta-\theta_0)}\, \mathrm{d}\theta_0 \qquad (r<a, -\pi \le \theta < \pi). \tag{3.23}$$

To derive a corresponding expression for the diffracted potential outside the arc we first decompose ϕ_d^α as

$$\phi_\mathrm{d}^\alpha(r,\theta) = \phi_\mathrm{c}^\alpha(r,\theta) + \phi_\mathrm{g}^\alpha(r,\theta) \quad \text{in } r>a, \tag{3.24}$$

where ϕ_c^α encompasses the scattering effect of the solid cylinder $B_0 = \{(r,\theta): r=a, \theta \in [-\pi,\pi)\}$, and ϕ_g^α is the potential instigated by the presence of the gap in the cylinder. The potential ϕ_c^α is such that the combination $\phi_\mathrm{i}^\alpha + \phi_\mathrm{c}^\alpha$ satisfies the Neumann boundary condition (2.5) on B_0. An explicit expression for ϕ_c^α is easily calculated as

$$\phi_\mathrm{c}^\alpha(r,\theta) = \sum_{n=-\infty}^{\infty} Z_n H_n(kr) e^{in(\theta-\alpha)} \tag{3.25}$$

where H_n denotes the Hankel function of the first kind (this is the only kind of Hankel function appearing so the superscript in the usual notation $H_n^{(1)}$ is omitted for convenience), and $Z_n = -i^n J_n'/H_n'$. The corresponding far-field diffraction behaviour is given by

$$\phi_\mathrm{c}^\alpha \sim \sqrt{\frac{2}{\pi kr}} F_\mathrm{c}(\theta,\alpha) e^{i(kr-\pi/4)}, \quad F_\mathrm{c}(\theta,\alpha) = \sum_{n=-\infty}^{\infty} Z_n e^{in(\theta-\alpha-\pi/2)} \tag{3.26}$$

as $kr \to \infty$.

A suitable expansion for ϕ_g^α is

$$\phi_\mathrm{g}^\alpha(r,\theta) = \sum_{n=-\infty}^{\infty} c_n H_n(kr) e^{in\theta} \qquad (r>a, -\pi \le \theta < \pi), \tag{3.27}$$

where the c_n are to be determined. Then, bearing in mind the decompositions (3.5) and (3.24), and also the fact that by construction the radial derivative of the combination $\phi_\mathrm{i}^\alpha + \phi_\mathrm{c}^\alpha$ vanishes on $r=a$, we see that

$$v^\alpha(\theta) = \frac{\partial \phi^\alpha}{\partial r}(a^+,\theta) \equiv \frac{\partial \phi_\mathrm{g}^\alpha}{\partial r}(a^+,\theta) = \sum_{n=-\infty}^{\infty} c_n k H_n' e^{in\theta}$$

for $-\pi \leq \theta < \pi$, from which, using the orthogonality of the complex exponentials, together with the boundary condition (2.5), we have

$$c_n = \frac{1}{2\pi k H_n'} \int_{-\theta_1}^{\theta_1} v^\alpha(\theta_0) e^{-in\theta_0} \, \mathrm{d}\theta_0 \qquad (n \in \mathbb{Z}) \tag{3.28}$$

and so (3.27) can be written as

$$\phi_{\mathrm{g}}^\alpha(r, \theta) = \sum_{n=-\infty}^{\infty} \frac{H_n(kr)}{2\pi k H_n'} \int_{-\theta_1}^{\theta_1} v^\alpha(\theta_0) e^{in(\theta-\theta_0)} \, \mathrm{d}\theta_0. \tag{3.29}$$

The corresponding far-field behaviour is

$$\phi_{\mathrm{g}}^\alpha \sim \sqrt{\frac{2}{\pi kr}} F_{\mathrm{g}}(\theta, \alpha) e^{i(kr-\pi/4)}$$

as $kr \to \infty$, where

$$F_{\mathrm{g}}(\theta, \alpha) = \sum_{n=-\infty}^{\infty} \frac{e^{in(\theta-\pi/2)}}{2\pi k H_n'} \int_{-\theta_1}^{\theta_1} v^\alpha(\theta_0) e^{-in\theta_0} \, \mathrm{d}\theta_0. \tag{3.30}$$

In equation (3.23) we have an expression for the solution ϕ^α within the arc, and a combination of equations (2.4), (2.6), (3.24), (3.25) and (3.29) provide a corresponding expression for the solution outside the arc. Now these two expressions are equated where their domains of dependence meet, on the line $r = a, -\theta_1 < \theta < \theta_1$, across which ϕ^α is continuous. The result can be arranged as

$$\sum_{n=-\infty}^{\infty} L_n \int_{-\theta_1}^{\theta_1} v^\alpha(\theta_0) e^{in(\theta-\theta_0)} \, \mathrm{d}\theta_0 = \sum_{n=-\infty}^{\infty} M_n e^{in(\theta-\alpha)} \qquad (-\theta_1 < \theta < \theta_1), \tag{3.31}$$

where

$$L_n = \frac{1}{2\pi k} \left(\frac{J_n}{J_n'} - \frac{H_n}{H_n'} \right) = \frac{i}{\pi^2 k^2 a J_n' H_n'} \qquad (n \in \mathbb{Z}) \tag{3.32}$$

and

$$M_n = i^n J_n + Z_n H_n = 2\pi k i^n J_n' L_n = \frac{2i^{n+1}}{\pi k a H_n'} \qquad (n \in \mathbb{Z}) \tag{3.33}$$

in which the final representation in each of (3.32) and (3.33) follows after use of a standard Wronskian result for Bessel functions (equation (9.1.16) in [20]).

13

Interchanging the order of summation and integration on the left-hand side of (3.31) allows it to be rewritten as the integral equation

$$\int_{-\theta_1}^{\theta_1} K(|\theta - \theta_0|) v^\alpha(\theta_0) \, \mathrm{d}\theta_0 = g^\alpha(\theta) \qquad (-\theta_1 < \theta < \theta_1), \qquad (3.34)$$

where

$$K(|\theta - \theta_0|) = \sum_{n=-\infty}^{\infty} L_n e^{in(\theta - \theta_0)}, \ g^\alpha(\theta) = \sum_{n=-\infty}^{\infty} M_n e^{in(\theta - \alpha)} \qquad (-\theta_1 < \theta, \theta_0 < \theta_1).$$

$$(3.35)$$

Using the standard large order asymptotic form of J_n and H_n (see e.g. equation (9.3.1) in [20]), we find that $L_n \sim a/n\pi$ for large $|n|$, so that the kernel K is logarithmically singular as $\theta - \theta_0 \to 0$.

Equation (3.34) can be decomposed into a series of 'modal' problems, precisely as we did to derive embedding formulae for the boundary-value problem in section 3.1.1. Thus if $g^n(\theta) = e^{in\theta}$ then the solution of (3.34) can be written as

$$v^\alpha(\theta) = \sum_{n=-\infty}^{\infty} M_n e^{-in\alpha} v^n(\theta) \qquad (3.36)$$

where

$$\int_{-\theta_1}^{\theta_1} K(|\theta - \theta_0|) v^n(\theta_0) \, \mathrm{d}\theta_0 = g^n(\theta) \qquad (-\theta_1 < \theta < \theta_1) \qquad (3.37)$$

for $n \in \mathbb{Z}$. Comparison of (3.30) and (3.36) shows that the far-field diffraction coefficient for ϕ_g can be written in terms of the v^n as

$$F_g(\theta, \alpha) = \sum_{m=-\infty}^{\infty} \frac{e^{im(\theta - \pi/2)}}{2\pi k H_m'} \sum_{n=-\infty}^{\infty} M_n e^{-in\alpha} \int_{-\theta_1}^{\theta_1} v^n(\theta_0) g^{-m}(\theta_0) \, \mathrm{d}\theta_0. \quad (3.38)$$

3.2.1. Embedding formulae for the integral equation

The kernel $K(|\theta - \theta_0|)$ defined in (3.35) is of 'difference' (or sometimes 'displacement') type, since it depends only on the combination $\theta - \theta_0$. It is well-known that equations containing such kernels admit embedding formulae (see, for example, [7]). The integral equation in (3.37) is actually of a very similar form to that investigated in [7], namely

$$\mu \phi_\alpha(x) - \int_0^1 \tilde{k}(x - x_0) \phi_\alpha(x_0) \, \mathrm{d}x_0 = e^{-i\alpha x} \qquad (0 < x < 1), \qquad (3.39)$$

in which $\alpha \in \mathbb{R}$ is a parameter, $\mu \in \mathbb{C}$ a given constant, and the kernel $\tilde{k}$ (denoted k in [7]) is at most weakly singular. Because the results in [7] we wish to adapt for our problem only make use of the fact that the implied integral operator in (3.39) is injective, rather than invertible, and the uniqueness of the solution to our underlying boundary-value problem certainly guarantees the injectivity of the integral operator in (3.34), we readily deduce, after appropriate changes to notation and integration interval, two results.

The first result can be written as

$$G_{p,-p}G_{n,m} = G_{p,m}G_{p,-n} - G_{p,-m}G_{p,n} \qquad (m \in \mathbb{Z}), \qquad (3.40)$$

for $n, p, m \in \mathbb{Z}$, with n and $\pm p$ distinct. Here

$$G_{n,m} = (n - m) \int_{-\theta_1}^{\theta_1} v^n(\theta)g^{-m}(\theta)\,\mathrm{d}\theta \qquad (n, m \in \mathbb{Z}) \qquad (3.41)$$

is a far-field diffraction coefficient-like quantity, and to derive (3.40) use has been made of both reciprocity and symmetry relations, respectively

$$G_{n,m} = G_{-m,-n} \qquad (n, m \in \mathbb{Z}) \qquad (3.42)$$

and

$$G_{n,m} = -G_{-n,-m} \qquad (n, m \in \mathbb{Z}), \qquad (3.43)$$

the latter following from

$$v^n(\theta) = v^{-n}(-\theta) \qquad (n \in \mathbb{Z}, \theta \in (-\theta_1, \theta_1)). \qquad (3.44)$$

Equation (3.40) expresses the far-field diffraction coefficient for v^n, $G_{n,m}$, in terms of quantities which require only knowledge of the particular solution v^p for their calculation, and thus is equivalent to the earlier formula (3.18). Verification of this relationship is straightforward: from (3.24), (3.25) and (3.29) we have

$$\phi_{\mathrm{d}}^\alpha(r, \theta) = \sum_{n=-\infty}^{\infty} H_n(kr)e^{in\theta} \sum_{p=-\infty}^{\infty} e^{-ip\alpha}\left(Z_p\delta_{pn} + \frac{M_p}{2\pi kH_n'}\int_{-\theta_1}^{\theta_1} v^p(\theta_0)e^{-in\theta_0}\,\mathrm{d}\theta_0\right),$$
$$(3.45)$$

and comparison of this with (3.9) shows that, in the notation of (3.12) and (3.41),

$$\hat{f}_{n,m} = \frac{e^{-i(n+m)\pi/2}M_n G_{n,m}}{2\pi kH_m'} \qquad (n, m \in \mathbb{Z}), \qquad (3.46)$$

15

from which the equivalence of (3.18) and (3.40) is readily confirmed.

Integrals of the form $\int_{-\theta_1}^{\theta_1} v^n(\theta_0)g^{-m}(\theta_0)\ \mathrm{d}\theta_0$ are required to evaluate the far-field coefficient $F_{\mathrm{g}}(\theta, \alpha)$ in (3.38), and from (3.40) and (3.41) they have the representation

$$\int_{-\theta_1}^{\theta_1} v^n(\theta_0)g^{-m}(\theta_0)\ \mathrm{d}\theta_0 = \frac{G_{p,m}G_{p,-n} - G_{p,-m}G_{p,n}}{(n-m)G_{p,-p}} \tag{3.47}$$

for distinct n, m. In the case $n = m$ we must use L'Hôpital's rule (as in section 3.1.1) to give

$$\int_{-\theta_1}^{\theta_1} v^m(\theta_0)g^{-m}(\theta_0)\ \mathrm{d}\theta_0 = \frac{-G_{p,m}\hat{G}_{p,-m} - G_{p,-m}\hat{G}_{p,m}}{G_{p,-p}} \tag{3.48}$$

where

$$\hat{G}_{p,m} = \frac{\partial}{\partial n}\left(G_{p,n}\right)\Big|_{n=m} = -\int_{-\theta_1}^{\theta_1} v^p(\theta_0)e^{-im\theta_0}\ \mathrm{d}\theta_0 - i(p-m)\int_{-\theta_1}^{\theta_1}\theta_0 v^p(\theta_0)e^{-im\theta_0}\ \mathrm{d}\theta_0. \tag{3.49}$$

Thus inserting (3.47) and (3.48) into (3.38) results in

$$\begin{aligned}
F_{\mathrm{g}}(\theta, \alpha) &= \sum_{m=-\infty}^{\infty}\frac{e^{im(\theta-\pi/2)}}{2\pi k H_m'}\sum_{n=-\infty,\neq m}^{\infty} M_n e^{-in\alpha}\left(\frac{G_{p,m}G_{p,-n} - G_{p,-m}G_{p,n}}{(n-m)G_{p,-p}}\right)\\
&\quad -\sum_{m=-\infty}^{\infty}\frac{e^{im(\theta-\pi/2)}}{2\pi k H_m'}M_m e^{-im\alpha}\left(\frac{G_{p,m}\hat{G}_{p,-m} + G_{p,-m}\hat{G}_{p,m}}{G_{p,-p}}\right)
\end{aligned} \tag{3.50}$$

which expresses the far-field diffraction coefficient $F_{\mathrm{g}}(\theta, \alpha)$ in terms of quantities which depend on the single modal solution v^p.

The second result which can be inferred from [7] was not derived in section 3.1. It relates the solutions of (3.37) themselves rather than their far-field diffraction coefficients:

$$G_{p,-p}v^n(\theta) = G_{p,n}[v^p(-\theta) - i(p+n)(V_{-n}v^p)(-\theta)] + G_{p,-n}[v^p(\theta) + i(p-n)(V_n^* v^p)(\theta)], \tag{3.51}$$

where we have introduced the Volterra integral operators

$$(V_n v)(\theta) = \int_{-\theta_1}^{\theta} v(\theta_0)e^{in(\theta-\theta_0)}\ \mathrm{d}\theta_0, \quad (V_n^* v)(\theta) = \int_{\theta}^{\theta_1} v(\theta_0)e^{in(\theta-\theta_0)}\ \mathrm{d}\theta_0 \tag{3.52}$$

16

for $n \in \mathbb{Z}$. Thus once the single solution v^p, of (3.37), is determined, (3.51) can be used to determine all others. Equation (3.36) can then in turn be used to construct v^α for any incident plane wave angle α, again in terms of the single solution v^p of the modal problem, as

$$
\begin{aligned}
G_{p,-p}v^\alpha(\theta) \;=\; & \sum_{n=-\infty}^{\infty} M_n e^{-in\alpha} G_{p,n}[v^p(-\theta) - i(p+n)(V_{-n}v^p)(-\theta)] \\
& + \sum_{n=-\infty}^{\infty} M_n e^{-in\alpha} G_{p,-n}[v^p(\theta) + i(p-n)(V_n^* v^p)(\theta)]. \quad (3.53)
\end{aligned}
$$

4. Numerical implementation

In this section we determine a numerical approximation to a solution v^p of the modal integral equation (3.37), from which approximations to the far-field diffraction coefficient-like quantities $G_{p,q}$ can be calculated; these are inserted into (3.50) to give an approximation to $F_\mathrm{g}(\theta, \alpha)$. This approximation is compared to the result of a direct approximation of the full integral equation (3.34).

4.1. Numerical approximation

To derive an approximate solution of the modal problem (3.37) (with n replaced by p for convenience) we use Galerkin's method in conjunction with the Rayleigh-Ritz approximation

$$
v^p(\theta) \approx \sum_{q=0}^{P} \lambda_q^p \chi_q(\theta) \tag{4.1}
$$

where $P \in \mathbb{N}_0$, the λ_q^p are constants to be determined, and the χ_q are trial-functions specified below. The λ_q^p are found by substituting (4.1) into (3.37), multiplying both sides by $\chi_l(\theta)$, and integrating in θ across $(-\theta_1, \theta_1)$, which results in

$$
\int_{-\theta_1}^{\theta_1} \int_{-\theta_1}^{\theta_1} K(|\theta - \theta_0|) \sum_{q=0}^{P} \lambda_q^p \chi_q(\theta_0) \chi_l(\theta) \, \mathrm{d}\theta_0 \, \mathrm{d}\theta = \int_{-\theta_1}^{\theta_1} g^p(\theta) \chi_l(\theta) \, \mathrm{d}\theta \tag{4.2}
$$

for $l = 0, \ldots, P$. For each p this is a system of $P + 1$ equations from which to calculate the $P + 1$ unknowns $\lambda_0^p, \ldots, \lambda_P^p$. We write this system as $A\mathbf{l}^p = \mathbf{r}^p$,

17

where A has (l, q)-th entry

$$A_{lq} = \int_{-\theta_1}^{\theta_1} \int_{-\theta_1}^{\theta_1} K(|\theta - \theta_0|)\chi_q(\theta_0)\chi_l(\theta)\, d\theta_0\, d\theta \qquad (l, q = 0, \ldots, P), \qquad (4.3)$$

$\mathbf{l}^p$ is a column vector with q-th entry λ_q^p $(q = 0, \ldots, P)$, and $\mathbf{r}^p$ is a column vector with l-th entry

$$r_l^p = \int_{-\theta_1}^{\theta_1} g^p(\theta)\chi_l(\theta)\, d\theta \qquad (l = 0, \ldots, P). \qquad (4.4)$$

The choice of trial-function is motivated by the corner condition (2.8), from which $v(\theta) = O((\theta_1 \mp \theta)^{-1/2})$ near $\theta = \pm\theta_1$. Consequently we choose

$$\chi_l(\theta) = \frac{T_l(\theta/\theta_1)}{\sqrt{\theta_1^2 - \theta^2}} \qquad (l = 0, \ldots, P) \qquad (4.5)$$

where T_l is the Chebyshev polynomial of the first kind. Use of trial functions of this form to approximate a function which is square-root singular at each end of an interval was used previously in [21]. From (4.4),

$$r_l^p = \int_0^\pi \cos(l\sigma)e^{ip\theta_1\cos\sigma}\, d\sigma = \pi i^l J_l(p\theta_1) \qquad (p \in \mathbb{Z},\ l = 0, \ldots, P), \qquad (4.6)$$

upon using a standard Bessel function identity (equation (9.1.21) in [20]).

From (3.35), and using (4.4) and (4.6),

$$
\begin{aligned}
A_{lq} &= \sum_{n=-\infty}^{\infty} L_n r_l^n r_q^{-n} \\
&= \pi^2 i^{l-q} \sum_{n=-\infty}^{\infty} L_n J_l(n\theta_1) J_q(n\theta_1) \\
&= \pi^2 i^{l-q} L_0 J_l(0) J_q(0) + \pi^2 i^{l-q}[(-1)^{l+q} + 1] \sum_{n=1}^{\infty} L_n J_l(n\theta_1) J_q(n\theta_1).
\end{aligned}
$$

$$(4.7)$$

The terms in the sum in (4.7) are $O(n^{-2})$ as $n \to \infty$, so the sum is slowly convergent. However, calculations can be speeded up, as follows. First we use the expansions (equations (2.17),(2.18) in [17])

$$\frac{J_n(z)}{J_n'(z)} = \frac{z}{n} + \frac{z^3}{2n^3} - \frac{z^3}{2n^4} + O(n^{-5}), \qquad \frac{H_n(z)}{H_n'(z)} = -\frac{z}{n} - \frac{z^3}{2n^3} - \frac{z^3}{2n^4} + O(n^{-5}),$$

for $n \to \infty$ and z fixed, to show that L_n defined in (3.32) has the behaviour

$$L_n = \frac{a}{n\pi} + \frac{k^2 a^3}{2n^3\pi} + O(n^{-5}) \qquad (4.8)$$

for large n. Then combining (4.8) and the standard large argument expansion of the Bessel function of the first kind shows that $L_n J_l(n\theta_1) J_q(n\theta_1) = \gamma_n(l, q) + O(n^{-4})$, where

$$\gamma_n(l, q) = \frac{a}{n^2\pi^2\theta_1} \left\{ \cos[2n\theta_1 - (l + q + 1)\pi/2] + \cos[(l - q)\pi/2] \right\}$$
$$- \frac{a}{4n^3\pi^2\theta_1^2} \left\{ (2q^2 + 2l^2 - 1)\sin[2n\theta_1 - (l + q + 1)\pi/2] + 2(q^2 - l^2)\sin[(l - q)\pi/2] \right\}.$$

$$(4.9)$$

We thus write the infinite sum in (4.7) as

$$\sum_{n=1}^{\infty} L_n J_l(n\theta_1) J_q(n\theta_1) = \sum_{n=1}^{\infty} [L_n J_l(n\theta_1) J_q(n\theta_1) - \gamma_n(l, q)] + \gamma(l, q), \qquad (4.10)$$

in which the sum can be evaluated accurately by truncating the sum at a finite value of n since the terms are $O(n^{-4})$ as $n \to \infty$. We truncate at $n = 1500$ for all calculations presented here, which is sufficient to ensure 5 decimal places of accuracy in approximations to A_{lq}. Also

$$\gamma(l, q) = \sum_{n=1}^{\infty} \gamma_n(l, q) = \frac{a}{2\pi^2\theta_1} \left(\lambda_2 + \bar{\lambda}_2 + \frac{\pi^2}{3}\cos[(l - q)\pi/2] \right)$$
$$- \frac{a}{8i\pi^2\theta_1^2} \left((2q^2 + 2l^2 - 1)(\lambda_3 - \bar{\lambda}_3) + 4i(q^2 - l^2)\zeta(3)\sin[(l - q)\pi/2] \right)$$

$$(4.11)$$

in which ζ denotes the zeta function, and $\lambda_j = e^{-i(l+q+1)\pi/2} \mathrm{Li}_j(e^{2i\theta_1})$ $(j = 2, 3)$ where

$$\mathrm{Li}_j(z) = \sum_{n=1}^{\infty} \frac{z^n}{n^j} = \frac{(-1)^{j-1}}{(j-2)!} \int_0^1 t^{-1} \ln^{j-2} t \ln(1 - zt) \, \mathrm{d}t$$

is the polylogarithm function (section 25.12, [22]), which can be evaluated accurately using standard quadrature techniques applied to its integral form.

Once the λ_q^p are determined, the far-field diffraction coefficient-like quantity for the modal problem, $G_{p,m}$ in (3.41), is approximated by

$$G_{p,m} \approx (p - m) \sum_{q=0}^{P} \lambda_q^p \, \overline{r_q^m}. \qquad (4.12)$$

19

To apply the embedding formula (3.40) when $n = m$ we also require an approximation to the modified coefficient $\hat{G}_{p,m}$ in (3.49), and for this we need

$$\int_{-\theta_1}^{\theta_1} \theta_0 v^p(\theta_0) e^{-im\theta_0} \, \mathrm{d}\theta_0 \approx \int_{-\theta_1}^{\theta_1} \theta_0 \sum_{q=0}^{P} \lambda_q^p \chi_q(\theta_0) e^{-im\theta_0} \, \mathrm{d}\theta_0$$

where

$$\int_{-\theta_1}^{\theta_1} \theta_0 \chi_q(\theta_0) e^{-im\theta_0} \, \mathrm{d}\theta_0 = \theta_1 \int_0^{\pi} \cos\sigma \cos(q\sigma) e^{-im\theta_1 \cos\sigma} \, \mathrm{d}\sigma = \frac{1}{2}\theta_1(\overline{r_{q+1}^m} + \overline{r_{q-1}^m}), \tag{4.13}$$

so that

$$\hat{G}_{p,m} \approx -\sum_{q=0}^{P} \lambda_q^p \left[\overline{r_q^m} + \frac{1}{2} i(p-m)\theta_1(\overline{r_{q+1}^m} + \overline{r_{q-1}^m}) \right]. \tag{4.14}$$

The approximation of the solution to the full problem (3.34) proceeds in a similar fashion, the only difference is in the right-hand side: g^α replaces g^p. We write

$$v^\alpha(\theta) \approx \sum_{q=0}^{P} \lambda_q^\alpha \chi_q(\theta) \tag{4.15}$$

where $\mathbf{l}^\alpha$, the vector with q-th entry λ_q^α, is found from $A\mathbf{l}^\alpha = \mathbf{r}^\alpha$, in which $\mathbf{r}^\alpha$ has q-th entry

$$r_q^\alpha = \int_{-\theta_1}^{\theta_1} g^\alpha(\theta) \chi_q(\theta) \, \mathrm{d}\theta = \int_{-\theta_1}^{\theta_1} \sum_{n=-\infty}^{\infty} M_n e^{in(\theta-\alpha)} \chi_q(\theta) \, \mathrm{d}\theta = \sum_{n=-\infty}^{\infty} M_n e^{-in\alpha} r_q^n, \tag{4.16}$$

from (3.35) and (4.4). The sum in (4.16) converges very rapidly. To see this first note that from (3.33), $M_{-n} = M_n$ for $n \in \mathbb{Z}$. Also, from (4.8), $L_n = O(n^{-1})$ as $n \to \infty$, and as a consequence of equation (9.3.1) in [20],

$$J_n'(z) \sim \frac{1}{z}\sqrt{\frac{n}{2\pi}}\left(\frac{ez}{2n}\right)^n$$

as $n \to \infty$ for fixed z. Putting these results together we deduce that M_n is $O(|n|^{-|n|-1/2})$ as $n \to \pm\infty$.

Clearly $\lambda_q^\alpha = \sum_{n=-\infty}^{\infty} M_n e^{-in\alpha} \lambda_q^n$, which is the discrete version of the linearity relationship (3.36). From (3.30), the corresponding approximation to the

20

far-field diffraction coefficient $F_{\mathrm{g}}(\theta, \alpha)$ is then

$$
\begin{aligned}
F_{\mathrm{g}}(\theta, \alpha) &\approx \sum_{m=-\infty}^{\infty} \frac{e^{im(\theta-\pi/2)}}{2\pi k H_m'} \sum_{q=0}^{P} \lambda_q^{\alpha} \overline{r_q^m} \\
&= \sum_{m=-\infty}^{\infty} \frac{e^{im(\theta-\pi/2)}}{2\pi k H_m'} \sum_{q=0}^{P} \sum_{n=-\infty}^{\infty} M_n e^{-in\alpha} \lambda_q^n \overline{r_q^m}. \qquad (4.17)
\end{aligned}
$$

In practice both infinite sums in (4.17) are truncated at the finite values $\pm N$.

4.2. Results

Tables 1 and 2 demonstrate the convergence of the numerical scheme for the modal problem. Table 1 displays values of $|G_{3,1}|$ calculated via (4.12) for $\theta_1 = \pi/5$, $ka = \pi, 2\pi, 3\pi$, and increasing P. For larger ka or $\theta_1 \gtrsim \pi/2$, higher values of P must be taken to achieve the same accuracy. In the latter case, the matching of solutions 'inside' and 'outside' the arc, as in section 3.2, makes less sense as a formulation; a preferable numerical approach is likely the hypersingular integral equation route of [23,18], though this is not pursued here. Table 2 lists values of $|G_{n,m}|$ for different n, m and increasing P, with $ka = 2\pi$ and $\theta_1 = \pi/5$. As n, m increase higher values of P are required to achieve the same accuracy.

The convergence of the numerical scheme for the full problem is demonstrated in Table 3. Displayed are values of the particular diffraction coefficient $|F_{\mathrm{g}}(\pi/3, \pi/7)|$, calculated via (4.17) for $ka = 2\pi$ and $\theta_1 = \pi/5$. Both infinite sums in (4.17) are truncated at $\pm N$, and values are shown in the table for increasing N and P. The convergence with P is comparable to that of the modal problem, and the factors of $1/H_m'$ ($= O(|m|^{-|m|+1/2})$ as $m \to \pm\infty$) and M_n in (4.17) guarantee rapid convergence of the sums in m and n respectively as the truncation parameter N is increased.

Now we implement the embedding formula via the representation (3.50). We solve the modal problem for v^p, approximate the required $G_{p,m}$ and $\hat{G}_{p,m}$ using (4.12) and (4.14), and then evaluate the right-hand side of (3.50), truncating the infinite sums at $\pm N$. The results of Table 2 indicate that the approximation to v^p converges most quickly for small values of p; for comparison we display in Table 4 results for $p = 1$ and also $p = 9$, for increasing N and P. As expected

the embedding formula results converge more slowly for the larger value of p, reflecting the slower convergence of the approximation to v^p in this case.

To demonstrate the utility of the embedding formula, figure 2(a) shows a contour plot of $|F_{\mathrm{g}}(\theta, \alpha)|$ for $-\pi \leq \theta, \alpha \leq \pi$, for parameter values $ka = 2\pi$ and $\theta_1 = \pi/5$. The reciprocity principle (2.10) and symmetry property (2.11) are responsible for the various symmetries. The results for the plot were generated by calculating only a single approximate solution v^1, and then using the embedding formula (3.50) to calculate all values of $|F_{\mathrm{g}}(\theta, \alpha)|$. Figure 2(b) shows values of $|F_{\mathrm{g}}(\theta, \alpha) + F_{\mathrm{c}}(\theta, \alpha)|$, which is the far-field diffraction coefficient stemming from the combined effect of the gap and the cylinder, the latter given in (3.26).

Finally we implement the embedding formula (3.53) which expresses v^α in terms of v^p. Figure 3(a) displays values of $v^\alpha(\theta)$ (multiplied by $\sqrt{\theta_1^2 - \theta^2}$, to avoid singular behaviour at the end-points) across the gap $-\theta_1 < \theta < \theta_1$, for parameter values $ka = 2\pi$, $\theta_1 = \pi/5$ and incident wave angle $\alpha = 2\pi/3$. Results from a direct calculation are shown as lines; the corresponding results from the embedding formula (3.53), with $p = 1$, are denoted by symbols, and as expected show excellent agreement with the direct results. Also shown, in figure 3(b), is a plot of $\mathrm{Re}(\phi^\alpha(x, y))$ for the same parameter values, calculated from an approximation to v^α using equations (2.4), (3.20), (3.25) and (3.27).

5. Conclusions and future directions

Based on a decomposition of the incident plane wave into an infinite sum of modes of the form $J_n(kr)e^{in\theta}$, for the first time embedding formulae for a simple polar geometry, consisting of a portion of the circular arc $r = a$, have been derived. Embedding formulae for the far-field diffraction coefficients have been derived directly from the boundary-value problem and from an integral equation formulation; the latter formulation also allowed the derivation of embedding formulae for the near-field solution. Numerical results confirm the accuracy and utility of the embedding formulae.

Dirichlet boundary conditions in place of Neumann conditions require little change. Embedding formulae for related but more complicated scatterers can

22

also be derived. Few modifications to the process are required if the circular arc contains more than one gap, or if multiple concentric punctured circular arcs are present (see figs. 4(a),(b)). In each of these cases the route which stems from the boundary-value problem will be the more straightforward to follow, as the integral equation formulations will be relatively complicated. The number of solutions required for the embedding formula will equal the total number of barrier tips in B; if B is symmetric around $\theta = 0$ then half as many solutions will be needed.

Perhaps more interesting is the case displayed in fig. 4(c), for which the new feature is the inclusion in the scatterer's boundaries of lines of the form $\theta = \text{constant}$. Why should this class of scattering geometry be amenable to the methods described in this paper? To answer this, we recall the portion of [9] which considered embedding formulae for scattering by a right-angled wedge, with faces $B_1 = \{(x, y) : x < 0, y = 0\}$ and $B_2 = \{(x, y) : x = 0, y < 0\}$. This was effected by noticing that the second-order differential operator $H_\alpha = \partial^2/\partial x^2 + k^2 \cos^2 \alpha I$ evidently commutes with the Helmholtz operator, annihilates the incident wave, preserves the radiation condition and boundary conditions on B_1, and, when applied to solutions of the Helmholtz equation $\partial^2 \phi/\partial x^2 + \partial^2 \phi/\partial y^2 + k^2 \phi = 0$, it also preserves boundary conditions on B_2, since

$$H_\alpha \phi = \frac{\partial^2 \phi}{\partial x^2} + k^2 \cos^2 \alpha \ \phi = -\frac{\partial^2 \phi}{\partial y^2} - k^2 \sin^2 \alpha \ \phi$$

in which the only differentiation is now directed along the face B_2. Embedding formulae for the right-angled wedge were then derived using this differential operator H_α.

These ideas can be carried over to our situation using the operator $D_n = \partial^2/\partial \theta^2 + n^2 I$ in place of H_α, which clearly commutes with the Helmholtz equation, annihilates the incident mode ϕ_i^n in (3.2), and preserves the radiation condition and the boundary condition on any boundary $r = \text{constant}$. The only question mark remaining concerns its maintenance of boundary conditions on

boundaries of the form $\theta = \text{const}$. But

$$D_n \phi^n = \frac{\partial^2 \phi^n}{\partial \theta^2} + n^2 \phi^n = n^2 \phi^n - \left(r^2 \frac{\partial^2 \phi^n}{\partial r^2} + r \frac{\partial \phi^n}{\partial r} + k^2 r^2 \phi^n \right),$$

in which the only differentiation is now directed along the boundary, so that D_n does indeed preserve homogeneous Neumann or Dirichlet boundary conditions on such boundaries. With the required properties of D_n having been established, the derivation of embedding formulae for the class of scatterers displayed in fig. 4(c) should be straightforward.

We note that the scatterers displayed in figs. 4(b),(c) take the form of splitring resonators (see, e.g. [24,25]). These structures are of interest since they can be used to construct so-called 'left-handed' media, i.e. media with a negative refractive index.

Lastly, it seems plausible that embedding formulae for multiple structures of the types displayed in figs. 1 and 4, which are centred at different points, could be derived. Whilst the methods presented in this paper certainly seemed to require the boundaries of the scatterer to each coincide with a portion of the line $r = \text{constant}$, the common use of Graf's addition formula (equation (9.1.79) in [20]) in problems involving scattering by multiple circular scatterers (see, e.g. [18],[26]) may be transferable. Further work is underway to investigate this possibility.

Acknowledgements

References

[1] M.H. Williams, Diffraction by a finite strip, Q. J. Mech. Appl. Math. 35 (1982) 103–124.

[2] D. Porter, K.-W.E. Chu, The solution of two wave-diffraction problems, J. Eng. Math. 20 (1986) 63–72.

[3] N.R.T. Biggs, D. Porter, D.S.G. Stirling, Wave diffraction through a perforated breakwater, Q. J. Mech. Appl. Math. 53 (2000) 375–391.

[4] N.R.T. Biggs, D. Porter, Wave diffraction through a perforated barrier of non-zero thickness, Q. J. Mech. Appl. Math. 54 (2001) 523–547.

[5] N.R.T. Biggs, D. Porter, Wave scattering by a perforated duct, Q. J. Mech. Appl. Math. 55 (2002) 249–272.

[6] C.M. Linton, Embedding formulas and singularities in acoustic scattering, in: Proceedings of IUTAM Symposium on Asymptotics, Singularities and Homogenisation in Problems of Mechanics, 2003, pp. 15–22.

[7] D. Porter, The solution of integral equations with difference kernels, J. Int. Eqns 3 (3) (1991) 429–454.

[8] R.V. Craster, A.V. Shanin, E.M. Doubravsky, Embedding formulae in diffraction theory, Proc. R. Soc. Lond. A 459 (2003) 2475–2496.

[9] R.V. Craster, A.V. Shanin, Embedding formulae for diffraction by rational wedge and angular geometries, Proc. R. Soc. Lond. A 461 (2005) 2227–2242.

[10] E.A. Skelton, R.V. Craster, A.V. Shanin, V. Valyaev, Embedding formulae for scattering by three-dimensional structures, Wave Motion, 47 (2010) 299–317.

[11] N.R.T. Biggs, A new family of embedding formulae for diffraction by wedges and polygons, Wave Motion, 43 (7) (2006) 517–528.

[12] E.A. Skelton, R.V. Craster, A.V. Shanin, Embedding formulae for diffraction by non-parallel slits, Q. J. Mech. Appl. Math. 61 (2008) 93–116.

[13] C.C. Mei, R.P. Petroni, Waves in a harbor with protruding breakwaters, J. Waterways Harbors Coastal Eng. Proc. ASCE 99 (1973) 209–229.

[14] T.L. Yip, T. Sahoo, A.T. Chwang, Wave oscillation in a circular harbor with porous wall, J. Appl. Mech. 68 (4) (2000) 603–607.

[15] B. Guizal, D. Felbacq, Numerical computation of the scattering matrix of an electromagnetic resonator, Phys. Rev. E 66 (2002) 026602.

[16] A. Burrows, Waves incident on a circular harbour, Proc. R. Soc. Lond. A 401 (1985) 349–371.

[17] C.M. Linton, Accurate solution to scattering by a semi-circular groove, Wave Motion 46 (2009) 200–209.

[18] C.M. Linton, P. McIver, Handbook of mathematical techniques for wave/structure interactions, Chapman & Hall CRC, 2001.

[19] D.S. Jones, Acoustic and Electromagnetic Waves, Oxford University Press, 1989.

[20] M. Abramowitz, I.A. Stegun, eds. Handbook of mathematical functions with formulas, graphs, and mathematical tables, New York: Dover Publications, 1964.

[21] R. Porter, D.V. Evans, Complementary approximations to wave scattering by vertical barriers, J. Fluid Mech. 294 (1995) 155–180.

[22] F.W.J. Olver, D.W. Lozier, R.F. Boisvert, C.W. Clark, eds. NIST Handbook of Mathematical Functions, Cambridge University Press, 2010.

[23] N.F. Parsons, P.A. Martin, Scattering of water waves by submerged plates using hypersingular integral equations, Appl. Ocean Res. 14 (1992) 313–321.

[24] A.B. Movchan, S. Guenneau, Split-ring resonators and localized modes, Phys. Rev. B 70 (2004) 125116.

[25] S.G. Llewellyn Smith, A.M.J. Davis, The split-ring resonator, Proc. R. Soc. Lond. A 466 (2010) 3117–3134.

[26] P.A. Martin, Multiple Scattering: Interaction of Time-Harmonic Waves with N Obstacles, Cambridge University Press, 2006.
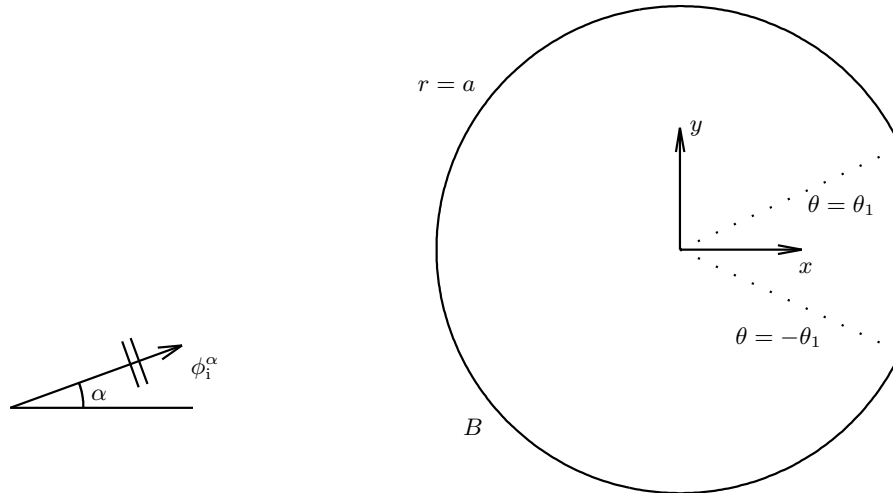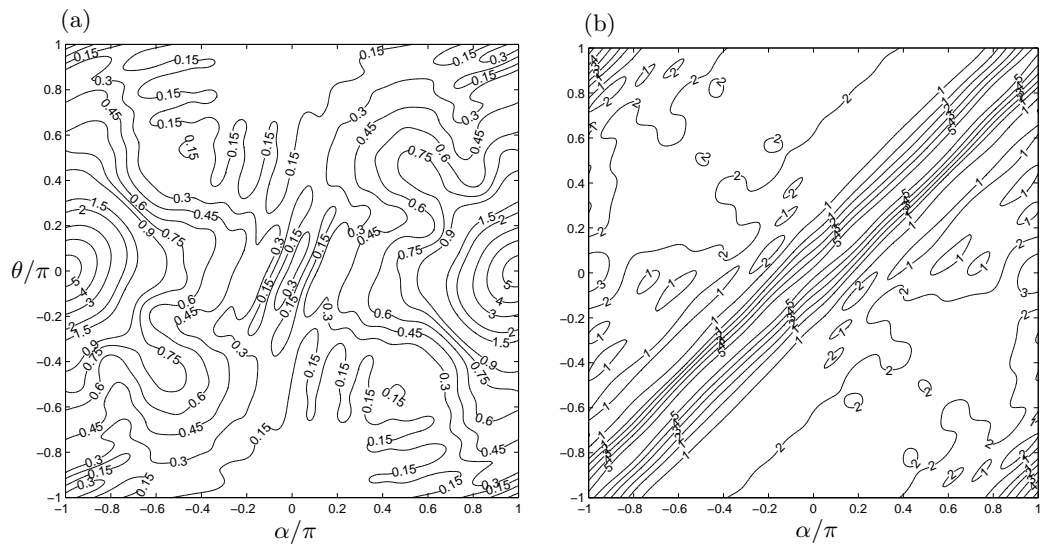
Figure 1: Geometry of scatterer B.

Figure 2: Absolute value of far-field diffraction coefficients, for $ka = 2\pi$ and $\theta_1 = \pi/5$, as functions of incident angle α and observation angle θ. Panels (a) and (b) display $|F_{\mathrm{g}}(\theta, \alpha)|$ and $|F_{\mathrm{g}}(\theta, \alpha) + F_{\mathrm{c}}(\theta, \alpha)|$ respectively.
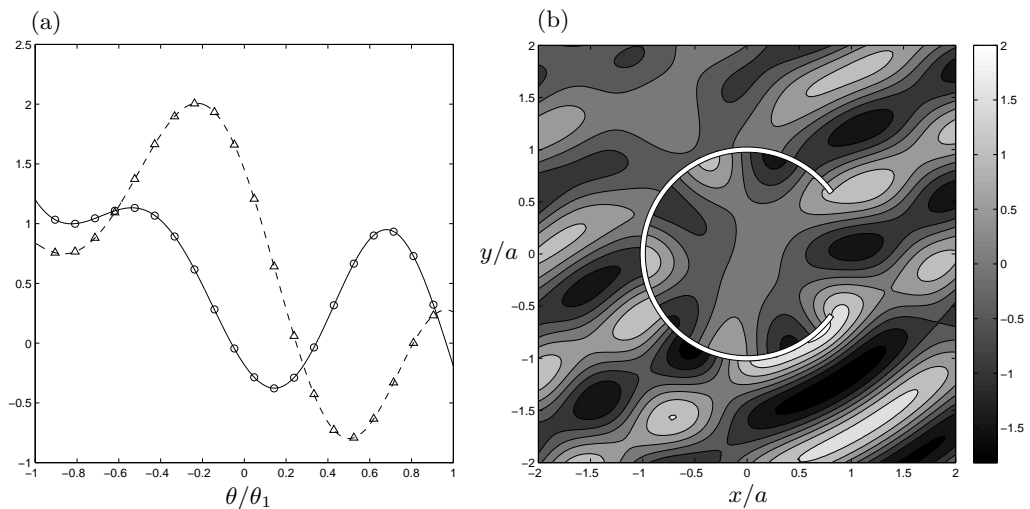
27

Figure 3: Panel (a) displays values of real part (solid line) and imaginary part (dashed line) of $v^\alpha(\theta)\sqrt{\theta_1^2 - \theta^2}$, for $ka = 2\pi$, $\theta_1 = \pi/5$ and incident wave angle $\alpha = 2\pi/3$. Symbols denote corresponding results from embedding formula (3.53), for $p = 1$. Panel (b) shows $\mathrm{Re}\{\phi^\alpha(x,y)\}$, for the same parameter values.
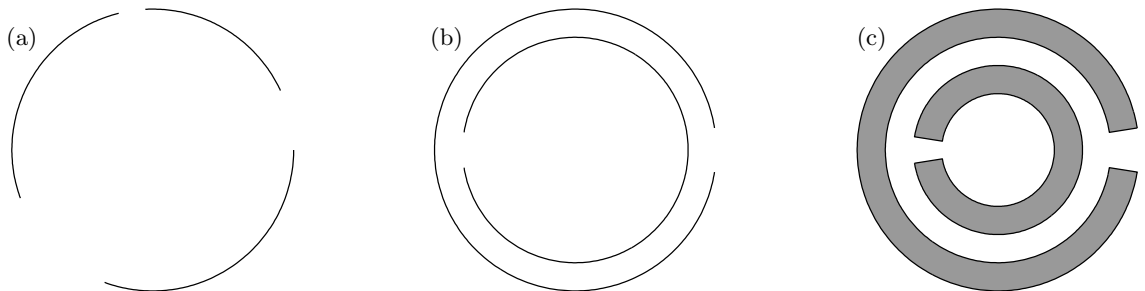

Figure 4: Examples of alternative scatterers B for which embedding formulae can be derived.

ka	P					
	2	4	6	8	10	12
π	2.33437	2.35708	2.35711	2.35711	2.35711	2.35711
2π	8.41238	8.42985	8.42994	8.42993	8.42993	8.42993
3π	11.66046	8.77025	8.62414	8.62052	8.62046	8.62046

Table 1: Values of $|G_{3,1}|$ for different ka and increasing P. The gap in the barrier occupies $|\theta| < \theta_1 = \pi/5$.

28

$|G_{n,m}|$	P					
	2	4	6	8	10	12
$|G_{1,2}|$	5.65247	5.69458	5.69455	5.69454	5.69454	5.69454
$|G_{1,9}|$	7.67423	5.47806	5.27293	5.26695	5.26691	5.26691
$|G_{8,9}|$	0.66926	2.47901	3.52477	3.59077	3.59186	3.59187

Table 2: Values of $|G_{n,m}|$ for different n,m and increasing P. Here $ka = 2\pi$ and $\theta_1 = \pi/5$.

N	P				
	2	4	6	8	10
5	0.09577	0.10130	0.10193	0.10193	0.10193
10	0.08158	0.23453	0.25443	0.25509	0.25510
15	0.08245	0.23517	0.25433	0.25488	0.25488
20	0.08245	0.23517	0.25433	0.25488	0.25488

Table 3: Values of $|F_{\mathrm{g}}(\pi/3, \pi/7)|$ calculated via (4.17) for $ka = 2\pi$, $\theta_1 = \pi/5$ and increasing P and truncation parameter N.

N,p	P				
	2	4	6	8	10
10,1	0.34132	0.25576	0.25527	0.25510	0.25510
15,1	0.34094	0.25552	0.25505	0.25489	0.25488
20,1	0.34094	0.25552	0.25505	0.25489	0.25488
10,9	0.20317	0.06232	0.24417	0.25522	0.25510
15,9	0.20258	0.06431	0.24426	0.25503	0.25488
20,9	0.20258	0.06431	0.24426	0.25503	0.25489

Table 4: Values of $|F_{\mathrm{g}}(\pi/3, \pi/7)|$ calculated via the embedding formula (3.50) with increasing truncation parameter N, in terms of v^p for $p = 1, 9$ calculated using different values of P. Here $ka = 2\pi$ and $\theta_1 = \pi/5$. The converged value is 0.25488 (5d.p.).